World Academy of Science, Engineering and Technology
International Journal of Aerospace and Mechanical Engineering
Vol:11, No:6, 2017

Damage Strain Analysis of Parallel Fiber Eutectic

Jian Zheng, Xinhua Ni, Xiequan Liu

***Abstract*—**According to isotropy of parallel fiber eutectic, the no-damage strain field in parallel fiber eutectic is obtained from the flexibility tensor of parallel fiber eutectic. Considering the damage behavior of parallel fiber eutectic, damage variables are introduced to determine the strain field of parallel fiber eutectic. The damage strains in the matrix, interphase, and fiber of parallel fiber eutectic are quantitatively analyzed. Results show that damage strains are not only associated with the fiber volume fraction of parallel fiber eutectic, but also with the damage degree.

***Keywords*—**Parallel fiber eutectic, no-damage strain, damage strain, fiber volume fraction, damage degree.

I. Introduction

RECENTLY, using combustion synthesis to fabricate eutectic composite ceramic, the ceramics had high performance, high reliability, and low cost. Directionally solidified eutectics contain a large amount of clean interfaces between two strongly-bonded phases with typical inter-phase spacing in the micron range, and these characteristics result in an improvement of some material properties. For instance, fibrous eutectics present a very high flexural, tensile strength, and high toughness at room and high-temperatures [1]-[3]. By using the laser heated floating zone method to prepare eutectics, Sayir and Farmer [4] found the microstructures and orientation relationship between the phases in the system varied as a function of composition and growth rate, and microstructures varied from lamellar eutectics to fibrous ones as growth rate was increased substantially. Solidification is a surface reaction whose rate depends on the degree of under-cooling that drives it, so high under-cooling degree introduces a high nucleation rate and high solidification rate. At the high cooling rate of the and the high under-cooling degree, the fibrous eutectics are obtained, and within the fibrous eutectics aligned nano/micron fibers are embedded and are nearly perpendicular to the growth orientation of the fibrous eutectic [5]. One of the most significant barriers to the increased use of eutectic composite ceramic is the inability to predict accurately eutectic damage.

To date, the damage research is focused on the long-fiber composites. Under a load, the debonding phenomenon appeared in the interface of long-fiber composites, and then the fiber fracture occurred in the debonding area. There is local plastic deformation in matrix near the fracture fiber [6], [7], which lead to the redistribution of micromechanical stress and strain, then damage occurs [8], [9]. The fiber distribution in the parallel fiber eutectic is similar to that of long-fiber composites. But, there is an interphase between fiber and matrix.

In order to analyze the damage evolution of parallel fiber eutectic, we need to obtain the micromechanical stress field and strain field. Based on the microstructure of the parallel fiber eutectic, the damage variable is introduced and the no-damage strains and in-damage strains in the parallel fiber eutectic are obtained, and the maximum strain value is determined.

Jian Zheng is with the Shijiazhuang Institute of Technology, Shijiazhuang, Hebei, China (corresponding author, phone: 0086-13703216137; e-mail: zhengj2020@163.com).

Xinhua Ni and Xiequan Liu are with the Shijiazhuang Institute of Technology, Shijiazhuang, Hebei, China (e-mail: jxxynxh@163.com, lxqnxh@163.com).

II. No-Damage Strain Field in Parallel Fiber Eutectic

The parallel fiber eutectic is transverse isotropic. There are five independent elastic constants [10]. The longitudinal elastic modulus $E_{11}=E_m/(1+h_{1111})$, the transverse elastic modulus $E_{22}=E_m/(1+h_{2222})$, the longitudinal shear modulus $\mu_{12}=\mu_{13}=E_m/(1+h_{1212})$, the transverse shear modulus $\mu_{23}=E_m/(1+h_{2323})$, the Poisson's ratio of longitudinal-transverse $\upsilon_{12}=\upsilon_{13}=(\upsilon_m-h_{2211})/(1+h_{1111})$. Among them, the E_m and υ_m are the elastic modulus and Poisson's ratio of the matrix in parallel fiber eutectic, respectively; h_{ijkl} is the dimensionless flexibility increment.

Obtained from each flexibility component, the flexibility tensor for no-damage eutectic is as:

$$\boldsymbol{S}=\begin{Bmatrix}\boldsymbol{S}_{11} & 0\\ 0 & \boldsymbol{S}_{22}\end{Bmatrix} \tag{1}$$

where,

$$\boldsymbol{S}_{11}=\begin{Bmatrix}\frac{1}{E_{11}} & -\frac{\upsilon_{12}}{E_{22}} & -\frac{\upsilon_{12}}{E_{22}}\\ -\frac{\upsilon_{12}}{E_{11}} & \frac{1}{E_{22}} & -\frac{\upsilon_{23}}{E_{22}}\\ -\frac{\upsilon_{12}}{E_{11}} & -\frac{\upsilon_{23}}{E_{22}} & \frac{1}{E_{22}}\end{Bmatrix},\quad \boldsymbol{S}_{22}=\begin{Bmatrix}\frac{1}{\mu_{12}} & 0 & 0\\ 0 & \frac{1}{\mu_{12}} & 0\\ 0 & 0 & \frac{1}{\mu_{23}}\end{Bmatrix},\quad \upsilon_{23}=\frac{E_{22}}{2\mu_{23}}-1.$$

In the no-damage state, there is no damage in eutectic. The local strain tensor in parallel fiber eutectic can be described as:

$$\boldsymbol{\varepsilon}^{l}=\boldsymbol{S}\boldsymbol{\sigma}^{l} \tag{2}$$

According to the constitutive relation, the no-damage strain field in parallel fiber eutectic is as:

$$\begin{cases} \varepsilon_{11} = \dfrac{1}{E_{11}}\sigma_{11} - \dfrac{\nu_{12}}{E_{22}}\sigma_{22} - \dfrac{\nu_{12}}{E_{22}}\sigma_{33} \\ \varepsilon_{22} = -\dfrac{\nu_{12}}{E_{11}}\sigma_{11} + \dfrac{1}{E_{22}}\sigma_{22} - \dfrac{\nu_{23}}{E_{22}}\sigma_{33} \\ \varepsilon_{33} = -\dfrac{\nu_{12}}{E_{11}}\sigma_{11} - \dfrac{\nu_{23}}{E_{22}}\sigma_{22} + \dfrac{1}{E_{22}}\sigma_{33} \end{cases} \tag{3}$$

III. Damage Strain Field in Parallel Fiber Eutectic

The damage variable is introduced because of the damage phenomenon in parallel fiber eutectic under loading, as in [11]. The parallel fiber eutectic is transverse isotropic so that one longitudinal damage variable and two transverse damage variables are defined which are correlated with principal stress. Among them, the longitudinal damage variable d_1 represents microcrack in the plane which is vertical to fiber, and the microcrack is correlated with elastic properties along the fiber longitudinal direction in the parallel fiber eutectic. And the transverse damage variable d_2 and d_3 represent microcrack in the plane which is parallel to fiber, and the microcrack is correlated with the elastic properties along the fiber transverse direction in the parallel fiber area of composite eutectic. The shear damage variable d_4 is correlated with shear stress τ_{12} and τ_{13}. Thus, the transverse shear damage is obtained by the coaxial of stress and strain. According to (1), the damage flexibility tensor of parallel fiber eutectic is obtained as:

$$\boldsymbol{S'} = \begin{Bmatrix} \boldsymbol{S'_{11}} & 0 \\ 0 & \boldsymbol{S'_{22}} \end{Bmatrix} \tag{4}$$

Among them, $\boldsymbol{S'_{11}}$ is the flexibility tensor which is correlated with principal stress, and $\boldsymbol{S'_{22}}$ is the flexibility tensor which is correlated with shear stress. In the isotropic plane, the no-damage elastic constant and damage variable at $\boldsymbol{e}_2$ are numerically equal to $\boldsymbol{e}_3$. The flexibility tensor which is correlated with principal stress expressed as:

$$\boldsymbol{S'_{11}} = \begin{Bmatrix} \dfrac{1}{(1-d_1)E_{11}} & -\dfrac{\upsilon_{12}}{E_{22}} & -\dfrac{\upsilon_{12}}{E_{22}} \\ -\dfrac{\upsilon_{12}}{E_{11}} & \dfrac{1}{(1-d_2)E_{22}} & -\dfrac{\upsilon_{23}}{E_{22}} \\ -\dfrac{\upsilon_{12}}{E_{11}} & -\dfrac{\upsilon_{23}}{E_{22}} & \dfrac{1}{(1-d_2)E_{22}} \end{Bmatrix} \tag{5}$$

Reference [12] shows that the stress and strain are coaxial in the isotropic plane, so the transverse shear modulus is expressed as:

$$\mu'_{23} = \frac{(\sigma^l_{33} - \sigma^l_{22})}{2(\varepsilon^l_{33} - \varepsilon^l_{22})} \tag{6}$$

Derivation of (3) shows that $\varepsilon'_{33} - \varepsilon'_{22} = \dfrac{1+\upsilon_{23}(1-d_2)}{E_{22}(1-d_2)}(\sigma'_{33} - \sigma'_{22})$, thus transverse shear modulus is associated with transverse damage variable as:

$$\mu'_{23} = \frac{E_{22}(1-d_2)}{2[1+\upsilon_{23}(1-d_2)]} \tag{7}$$

μ'_{12} and μ'_{13} which are longitudinal shear moduli in the transversely isotropic plane are equal. The flexibility tensor about shear stress is as:

$$\mathbf{S}'_{22} = \begin{Bmatrix} \dfrac{1}{(1-d_3)\mu_{12}} & 0 & 0 \\ 0 & \dfrac{1}{(1-d_3)\mu_{12}} & 0 \\ 0 & 0 & \dfrac{2[1+\upsilon_{23}(1-d_2)]}{E_{22}(1-d_2)} \end{Bmatrix} \tag{8}$$

Reference [13] shows that damage first occurs in the matrices near the interface, and the form of damage is arc-microcracks occurring at the interface and then extending along the fiber interface. These microcracks have a slight effect on the damage along the vertical direction of fiber in the matrix of parallel fiber eutectic, and have a great influence on the damage along the transverse direction of fiber. Thus, d_1=0. The separation of largest crack area around fiber of the parallel fiber eutectic shows semicircular cylinder area, which is similar to the matrix spread by parallel fibers. According to [14], the maximum d_2 is shown as:

$$d_{2max} = \sqrt{\frac{4f_b}{\pi}} \tag{9}$$

where f_b is the fiber volume fraction of parallel fiber eutectic. The cylinder whose radius is A, is extracted from parallel fiber eutectic, in order to analyze shear damage variable. There is a fiber whose radius is a_0 and length is 2l along the central axis of the cylinder as shown Fig. 1.

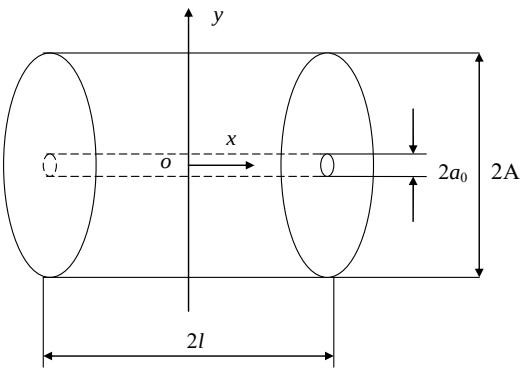

Fig. 1 Fiber in the parallel fiber eutectic

When the arc-crack appeared on the two-phase interface, and the maximum debonding area reached half cylinder, based on the equilibrium condition of shear lag analysis [15], the shear stress of half cylinder surface connected with the fiber should be equal to the shear stress of cylinder surface in any ring layer whose radius is *a*, that is:

$$\pi a_0 \tau_t' = 2\pi a \tau \tag{10}$$

where τ_t' is the shear stress along the fibers of half cylinder surface connected to the fiber, τ is the shear stress of cylinder surface in the ring layer whose radius is *a*. Based on Hooke's law: $\tau = \mu_m \frac{du}{da}$, in which *u* is the displacement along the fibers of matrix whose radius of cylinder surface is *a*. μ_m is the shear modulus of the matrix. $\frac{du}{da} = \frac{\tau_t' a_0}{2\mu_m a}$ can be obtained after the calculation of the simultaneous equations. The integral of the formula is shown in (11):

$$\int_{u_n}^{u_R} du = \frac{\tau_t' a_0}{2\mu_m} \int_{a_0}^{R} \frac{da}{a} \tag{11}$$

Result calculated from (11) is shown in (12):

$$\tau_t' = \frac{2\mu_m (u_R - u_n)}{a_0 \ln(R/a_0)} \tag{12}$$

where u_R is the matrix axial displacement and u_n is the fiber axial displacement. The shear stress of interface at the maximum damage is expressed in (10). When the interface has no damage, (10) can be transformed into $2\pi a_0 \tau_t = 2\pi a \tau$ where $\tau_t = \frac{\mu_m (u_R - u_n)}{a_0 \ln(R/a_0)}$ can be obtained by the use of the same method. According to $\tau_{tmax}' = 2\tau_t$ and (9), the maximum shear damage variable is:

$$d_{3\max} = 1/2 \tag{13}$$

The constitutive relations of parallel fiber eutectic can be expressed as shown in (14):

$$\boldsymbol{\varepsilon}' = \mathbf{S}'\boldsymbol{\sigma}' \tag{14}$$

Based on the constitutive relations in (14), the damage strain fields in parallel fiber eutectic are shown in (15):

$$\begin{cases} \varepsilon_{11}' = \frac{1}{E_{11}}\sigma_{11}' - \frac{\nu_{12}}{E_{22}}\sigma_{22}' - \frac{\nu_{12}}{E_{22}}\sigma_{33}' \\ \varepsilon_{22}' = -\frac{\nu_{12}}{E_{11}}\sigma_{11}' + \frac{1}{(1-d_2)E_{22}}\sigma_{22}' - \frac{\nu_{23}}{E_{22}}\sigma_{33}' \\ \varepsilon_{33}' = -\frac{\nu_{12}}{E_{11}}\sigma_{11}' - \frac{\nu_{23}}{E_{22}}\sigma_{22}' + \frac{1}{(1-d_2)E_{22}}\sigma_{33}' \end{cases} \tag{15}$$

The above equations show that damage strains are not only associated with the five independent elastic constants of parallel fiber eutectic, but also with the damage variable.

For parallel fiber eutectic, the material constants in the matrix and fiber are E_m=402 GPa, υ_m=0.233, E_b=233 GPa, υ_b = 0.31. The thickness of the interphase is Δ=1 nm. $f_a = \frac{4\Delta}{2\Delta + d} f_b$. If a tensile stress $\boldsymbol{\sigma}$ is forced along eutectic axis, the diameter of fiber is set at 125 nm. When d_2 is set to 1/3, 2/3 and 1 times of the maximum, the relationship between the strain components in matrix and fiber volume fraction f_b is shown in Figs. 2 and 3.

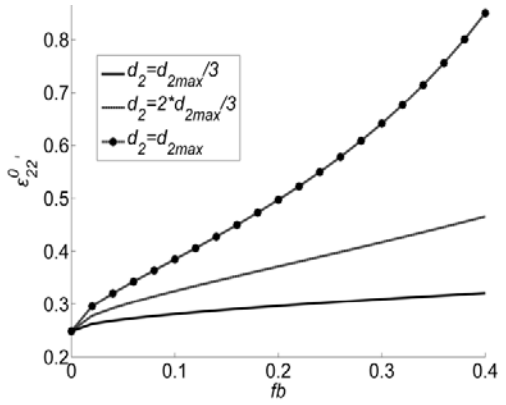

Fig. 2 Relationship between the strain in matrix parallel to eutectic axis and fiber fraction

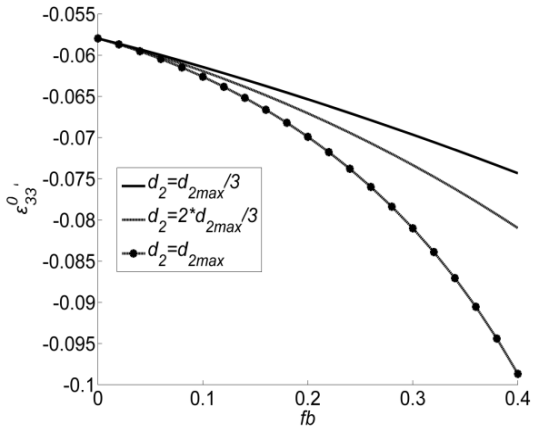

Fig. 3 Relation between traverse strain in matrix and fiber fraction

According to Fig. 2, the strain of matrices along the eutectic axis increases with the increase of fiber volume fraction. Fig. 3

shows that the traverse strain in matrix decreases with the increase of fiber volume fraction.

The diameter of fiber is set at 125 nm. When d_2 is set to 1/3, 2/3, and 1 times of the maximum, the relationship between the strain components in interphase and fiber volume fraction f_b is shown in Figs. 4 and 5.

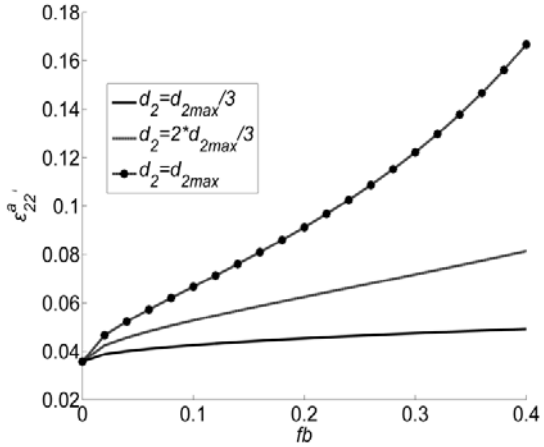

Fig. 4 Relationship between the strain in interphase parallel to eutectic axis and fiber fraction

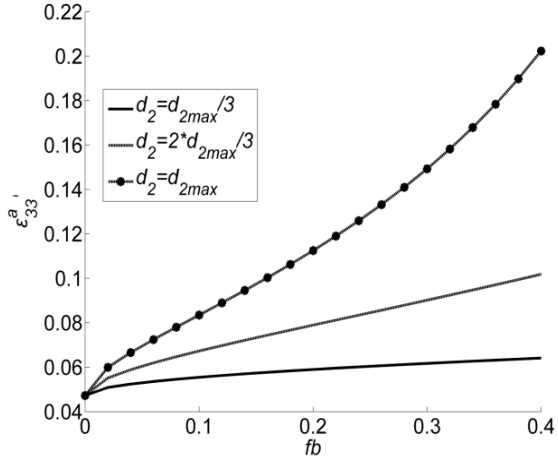

Fig. 5 Relation between traverse strain in interphase and fiber fraction

Figs. 4 and 5 show that the strain components in interphase increase with the increase of fiber volume fraction. The diameter of fiber is set at 125 nm.

When d_2 is set to 1/3, 2/3, and 1 times of the maximum, the relationship between the strain components in fiber and fiber volume fraction f_b is shown in Figs. 6 and 7.

Figs. 6 and 7 show that the strain components in fiber increase with the increase of fiber volume fraction.

Comparing Figs. 2 and 7, the maximum linear strain of matrix along the eutectic axis is the main factor of the matrix damage.

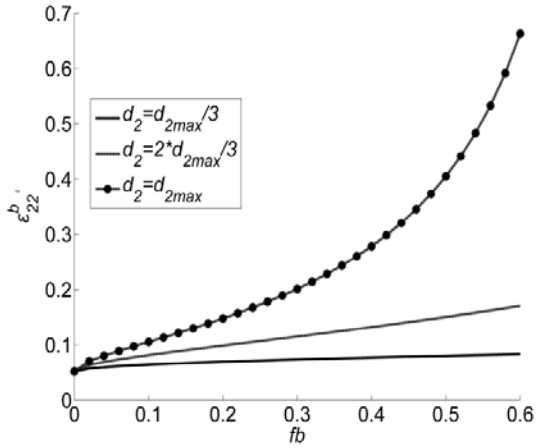

Fig. 6 Relationship between the strain in fiber parallel to eutectic axis and fiber fraction

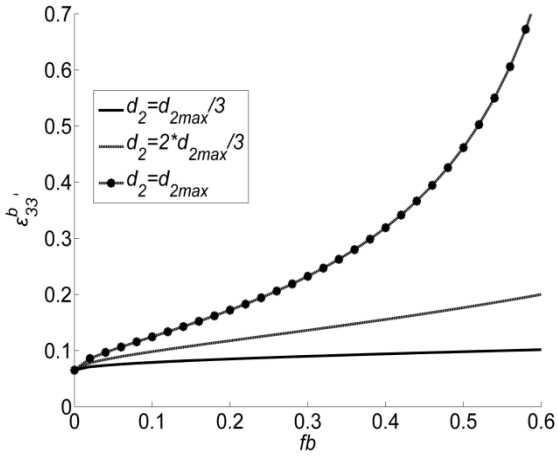

Fig. 7 Relation between traverse strain in fiber and fiber fraction

IV. Conclusion

1) The theoretical analysis indicates that damage strains are not only associated with the five independent elastic constants of parallel fiber eutectic, but also with the damage variable.
2) The damage strain of matrix in eutectic along the eutectic axis increases with the increase of fiber volume fraction, and the traverse strain of matrix decreases with the increase of fiber volume fraction. The greater the change of damage degree, the more intense the change of damage strains of matrix is.
3) The strain components of interphase in eutectic increase with the increase of fiber volume fraction, and the greater the change of damage degree, the more intense the change of damage strains of interphase is.
4) The axial and traverse damage strains of fiber in eutectic increase with the increase of fiber volume fraction, and the greater the change of damage degree, the more intense the change of damage strains of fiber is.

Acknowledgment

Jian Zheng thanks for the support of National Natural

Science Foundation of China (Grant No. 11272355).

REFERENCES

[1] C. Baudin, and M. H. Sayir, "Failure Mechanisms in Directionally Solidified Alumina-titania Composite", *Key Engineering Materials*, vol. 290, 2005, pp. 199–233.

[2] A. Sayir, M. H. Berger, and C. Baudin, "Microstructural and Mechanical Properties of Directionally Solidified Ceramic in Al_2O_3-Al_2TiO_3 Sysitems", Ceramic Enigineering & Science Proceeding, vol. 2, 2005, pp.225–233.

[3] J. Echigoya, "Structure of Interface in Directionally Solidified Oxide Eutectic Sysitems", *Jouenal of the European Ceramics Society*, vol. 8, 2005, pp. 1381–1387.

[4] A. Sayir, S. C. Farmer, "The Effect of the Microstructure on Mechanical Properties of Directionally Solidified $Al_2O_3/ZrO_2(Y_2O_3)$ Eutectic", *Acta mater.*, vol. 48, 2000, pp. 4691–4697.

[5] Z. M. Zhao, L. Zhang, Y. G. Song, "Microstructures and properties of rapidly solidified Y_2O_3 doped Al_2O_3/ZrO_2 composites prepared by combustion synthesis", *Scripta Materialia*, vol. 55, 2006, pp. 819–822.

[6] J. Q. Zhang, J. Wu, S. L. Liu, "Cyelically thermo-mechanical plasticity analysis for a broken fiber in ductile matrix composites using shear lag model", *Composites Science and Technology*, vol. 62, 2002, pp. 641–654.

[7] X. D. Zhi, J. M. Wu, F. FAN, "Failure of single-layer reticulated cylindrical shells subjected to earthquakes", *Chinese Journal of Computational Mechanics*, vol. 25, 2008, pp. 770–773.

[8] R. Talreja, "A conceptual framework for interpretation of MMC fatigue", *Materials Science and Engineering*, vol. A200, 1995, pp. 21–28.

[9] J. Liu, Y. M. Li, F. P. Zhang, "Effect of strain softening on delamination tip-field in composite laminate", *Chinese Journal of Computational Mechanics*, vol. 23, 2006, pp. 387–362.

[10] B. F. Li, J. Zheng, X. H. Ni, "Mechanical Properties of Composite Ceramic with Triangular Symmetrical Eutectic Colony", *Chinese Journal of Applied Mechanics*, vol. 29, 2012, pp. 127–132.

[11] X. C. Jiang, H. P. Xie, H. W. Zhou, "Analysis of Relationship between Macroscopic Damage Variable and Mesoscopic Damage Variable of quasi-brittle Materials under Compression", *Rock and Soil Mechanics*, vol. 9, 2008, pp. 2531–2536.

[12] P. Maimi, and J. A. Mayugo, "A Three-dimensional Damage Model for Transversely Isotropic Composite Laminates", *Journal of Composite Materials*, vol. 42, 2008, pp. 2717–2745.

[13] X.H. Ni, J. Zheng, X. Q. Liu, "Strength Model of Eutectic Ceramic Composite", *Chinese Journal of Solid Mechanics*, vol. 30, 2009, pp. 116–121.

[14] T. Sun, X. H. Ni, B. H. Han, "Analysis of damage strain field for ceramic composite with eutectic interphases", *Chinese Journal of Computational Mechanics*, vol. 29, 2012, pp. 527–531.

[15] X. Q. Liu, X.H. Ni, Y.T. Liu, "Mesomechanical Strength Model of Nano-Fibers Composite Ceramics", *Solid State Phenomena,* Vols. 121-123, 2007, pp. 1157–1160.